Journal of King Saud University – Science 34 (2022) 102328

HOSTED BY

Contents lists available at ScienceDirect

Journal of King Saud University – Science

journal homepage: www.sciencedirect.com

Original article

Translocation of pro-apoptotic proteins through basements membrane and hemidesmosome in the corneal epithelium of the keratoconus subjects

Ramachandran Samivel [a], Saud A. Alanazi [a], Ibraheem S. Almahuby [b], Adnan A. Khan [a], Omar Kirat [c], Essam S. Almutleb [b], Ali M. Masmali [a,*]

[a] Cornea Research Chair, Department of Optics and Vision Science, College of Applied Medical Sciences, King Saud University, Riyadh, Saudi Arabia
[b] Department of Optics and Vision Science, College of Applied Medical Sciences, King Saud University, Riyadh, Saudi Arabia
[c] Department of Ophthalmology, King Khalid Eye Specialist Hospital, Riyadh, Saudi Arabia

ARTICLE INFO

Article history:
Received 20 April 2022
Revised 28 June 2022
Accepted 14 September 2022
Available online 19 September 2022

Keywords:
Human corneas
Kerotoconus
Hemidesmosomes
Corneal epithelial basal cells
Basement's membrane
Pro-apoptosis

ABSTRACT

Keratoconus (KC) is an ectatic corneal disorder to frequently characterize by corneal thinning and severe visual impairment, and it continues to be one of the leading indications for corneal transplantation. The etiology is multi-factorial and pathological changes have been observed in the KC corneas. It is still unknown where the disease originates, but the changes in the corneal epithelium are considered to start even before a clinical sign appears. The present study, we investigated the potential role of basement membrane and hemidesmosomes damage whether they are participating a key role on pro-apoptotic protein elevations in the KC corneal epithelium. Samples of corneal epithelium from three KC and three normal subjects were used by Western blot, electron microscopy, immunohistochemistry and fluorescent staining. The histology and ultrastructural changes in the KC corneal sections were illustrated that arises the damage to the bowmen's layer, hemidesmosomes, and basement membrane broken. The basal cells of the corneal epithelium in KC exhibits squamous cells with absence of nuclei compared to the corneal epithelium of normal subjects. The expression of pro-apoptotic proteins Bax, phospho-p53, and cleaved caspase-3 were elevated significantly in the KC cornea when compared to normal corneal tissues extracts. Similarly, immunohistochemistry and triple antibodies staining (Bax, phosphor-p53, and cleaved caspase-3) of KC subjects were demonstrated an identical result as compared to the normal corneal sections. The Nile red/DAPI stain results correspondingly illustrated that KC corneas had less membrane lipid contents, and occurs a fewer progenitor cells than peripheral corneas in the normal subjects. Hence, the collective results indicate the colocalization of pro-apoptotic proteins transduced through basal epithelial cell damage and fragmented basement membrane, which is boost apoptotic induction in the KC corneal epithelium.

Abbreviations: KC, Keratoconus; EP, Epithelium; BM, Basement membrane; BC, Basal epithelial cells; BL, Basal layer; ST, Stroma; HD, Hemidesmosome; KR, Keratocyte; TEM, Transmission electron microscopy; BAX, Bcl-2-associated X protein; BAD, BCL2 associated agonist of cell death (BAD) protein; BID, BH3-interacting domain death agonist; Pp53, Phosphor tumor protein p53; Ccap-3, Cleaved caspase-3; DAPI, 4′,6-diamidino-2-phenylindole; PI, Propidium Iodide; PVDF, polyvinylidene fluoride membrane; HRP, Horseradish Peroxidase; PBST, Phosphate-Buffered Saline/Tween; TBST, Tris-Buffered Saline/Tween.

* Corresponding author at: Cornea Research Chair, Building No 24, Department of Optics & Vision Science, College of Applied Medical Sciences, King Saud University PO Box 10219, Riyadh 11433, Kingdom of Saudi Arabia.
E-mail address: amasmali@ksu.edu.sa (A.M. Masmali).

Peer review under responsibility of King Saud University.

Production and hosting by Elsevier

https://doi.org/10.1016/j.jksus.2022.102328

1. Introduction

In keratoconus (KC), corneal thinning and keratectasia are the most common symptoms, resulting in severe vision impairment and corneal swelling due to structural disintegration. Keratoconus usually affects one or both eyes bilaterally and generally asymmetrically (Amit et al., 2020). Globally, the incidence of KC ranges from approximately 1:400 to 1:2000 people suffered per annum. In a general population, KC has been reported to affect up to 2.34 % of individuals, 6–10 % of people with KC have a pattern of autosomal dominant inheritance with incomplete penetrance (Atilano et al., 2019; Chaerkady et al., 2013). The KC affects both genders from puberty to early mid-life, therefore it poses a significant socioeconomic burden to the society for both young and working individuals (Yam et al., 2019). Eventually, this causes irregular astigmatism and corneal fibrosis with significant vision loss (Hashmani et al., 2017). There is a very variable and unpredictable progression rate between patients following diagnosis, which can last up to two decades after presentation (Vazirani & Basu, 2013). Studies have concerned, that this prevalence is much higher due to improvements in corneal topography, allowing for earlier diagnosis of KC subjects (Masiwa and Moodley, 2020; Atalay et al., 2021; Li et al., 2021).

The histological examination of KC corneas reveals that changes are primarily noted in the epithelium, Bowman's layer, and the stroma (Kenney et al., 1997). But, the initial changes may occur either in the epithelium or stroma remains unclear. The KC corneas have been studied histopathological for fragmentation of the epithelial basement membrane (EBM), superficial linear ruptures in Bowman's layer filled with fibrotic connective tissue, and folds on Descemet's membrane (Marino et al., 2017). During early histopathological investigations, abnormalities in the corneal epithelium were noted, and it was postulated that insults to the epithelium caused proteolytic enzyme release, which caused stromal tissue degradation and an ensuing chain of events (Khaled et al., 2017).

Epithelium on the cornea is the outermost layer that acts as a physical barrier to protect pathogens and is in constant contact with tear film. There are distinguished three cellular layers in the epithelium: basal cells, wing cells and superficial cells (Kammergruber et al., 2019). As new epithelial cells are continually being generated at the basal level from the limbus, the corneal epithelium constantly renews itself. The wing cells migrate interiorly towards the cornea to form the superficial squamous cells, which eventually lose their adhesions (desmosomes) and slough off into the tear film (Mobaraki et al., 2019). Continuous loss of epithelium causes keratocyte apoptosis, and an abnormal epithelium might therefore impair collagen synthesis and keratocyte functions (You et al., 2018). Numerous pathological conditions can disrupt the many components that promote corneal epithelium damage. There are several abnormal morphologies of this highly dynamic tissue in KC including epithelial thinning, elongated basal epithelial cells, and breaks in the basement membrane (Grieve et al., 2016).

Moreover, KC has caused extensive oxidative damage to cornea, cultured cells, and tears in numerous molecular and biochemical findings (Atilano et al., 2019). The current therapeutic strategies are focused on lessening oxidative damage in corneal epithelial cells and preventing cell death. Previous studies have shown that oxidative stress plays a pivotal role in corneal epithelial cell apoptosis and KC occurrence (Liu and Yan, 2018; Chwa et al., 2006; Wojcik et al., 2013). *Ex vivo* studies and *in vitro* cultured cells have suggested the pathogenic mechanisms for KC, however the molecular pathology is not completely understood (Shetty et al., 2017; Kaluzhny et al., 2020). A therapeutic target for KC does not yet exist because the disease progression is still not fully studied. Among these phenomenon's, the epithelial cells have been increasingly targeted with key factors that enhance KC-associated damage in corneal integrity. Hence, the present study examined the effects of basement membrane and basal epithelia in KC subjects, whether they delivering proapoptotic factor transductions on peripheral and center corneal epithelium.

2. Materials and methods

2.1. Tissue collection

Human keratoconus (KC) corneal buttons of 8 mm diameter were obtained from the surgeon of King Khalid Eye Specialist Hospital (KKESH) from 3 subjects (aged 20 to 30 years; KC grade 3 and 4), As previously described in our laboratory study (Alkanaan et al., 2019). A total of three normal corneoscleral rims were procured from Timestrip Plus Company (Oklahoma Lions Eye Bank, LN, USA). During the tissue procurement and use process, the Declaration of Helsinki and local ethical regulations were followed. The ethics committees at both King Saud University and King Khaled Eye Specialist Hospital (Riyadh, Saudi Arabia) approved efficacy and safety of the study.

2.2. The process of preparing tissues for H&E staining

The KC and normal corneal tissues were dissected and harvested in a tissue culture hood. Each corneal button was cut into two halves, the first half was cut into two quarters, and the second half was collected and stored at −80 °C for immuno-blatting. The first quarter of the corneal tissue was prepared for electron microscopy by fixing it in 2.5 % glutaraldehyde with 0.1 M phosphate buffer. The second quarter of corneal tissue was fixed overnight in 10 % formalin (FA) in PBS, and then dehydrated and paraffin embedded. Sections of deparaffinized and rehydrated tissues (5-μm thickness) were stained with Hematoxylin & Eosin dyes and viewed under Olympus BX51 bright field microscopy using Cell Sensentry software.

2.3. Quantification of immunoblotting

The total proteins were extracted and protein concentrations were determined using Pierce Rapid Gold BCA protein assay kit (A53225; Thermo Scientific, UK). The total protein lysates (30 μg per each well) were loaded and subjected to 10–12 % SDS-PAGE before being electro-transferred to PVDF at 23 V for 10 min. The membrane was blocked with 5 % nonfat milk in Tris-buffered saline supplemented with 0.05 % Tween-20 at 37 °C for 1 h and incubated with primary antibodies Bax (mouse, #89477S), Bid (rabbit, #2002T), Bad (rabbit, #9239T), Phosphor-p53 (mouse, #9286T), cleaved caspase-3 (rabbit, #9664T), and anti-β-actin HRP (mouse, #12620S; 1:1000 Cell Signaling (USA)), overnight at 4 °C. The membranes were incubated with horseradish peroxide-conjugated anti-rabbit (#7074P2) and anti-mouse IgG (#7076P2) secondary antibodies (1:2000, Cell Signaling, USA) at room temperature for 2 h. After extensive washing with TBST buffer, the membrane was developed using chemiluminescent detection kit (WesternSure Premium, LI-COR, USA). The images were captured using a LI-COR C-DiGit Blot Scanner (Odyssey, LI-COR, USA) and quantified by using image J analysis software (NIH, Bethesda, MD).

2.4. Immunohistochemical staining

Immuno-staining of corneal tissue sections fixed and embedded in paraffin was performed using an indirect immunoperoxidase

method with antibody staining. The, 5-μM thickness paraffin tissue sections were incubated with appropriate primary antibodies at overnight, after deparaffinization and antigen retravel. After being washed for 3 times, the tissue sections were incubated with HRP-conjugated secondary antibody at room temperature for 1 h. Finally, the slides were conducted with DAB substrate working solution and photographed with a light microscope (Olympus BX51) connected with Cell Sensentry software.

2.5. Fluorescence microscopy staining

The Nile red/DAPI dual staining procedure was carried out according to the previously described method, with minor modifications (Jumabay et al., 2010). Briefly, the sections were deparaffinized, rehydrated, and washed with PBS buffer for 5 min each. The slides were incubated in Nile red (1 μg/mL) with PBS buffer (Sigma Aldrich, St Louis, MO, USA) for 30 min at room temperature, then washed for 5 min in water. The sections were stained with 4′,6-Diamidine-2′-phenylindole dihydrochloride (DAPI) in PBS (2 μg/mL) and incubated in the dark for 15 min. After that, cells were washed in PBS, and morphology was examined with blue (ex/em: 358/461 nm) and red (ex/em: 586/617 nm) filters in fluorescence microscopy (BX53 Olympus, Germany). Photographs were captured with using BX53 microscope equipped with a CCD cooled camera. The images were merged using Cell Sensentry software.

2.6. Electron microscopy

The KC and normal corneal tissues were fixed in 2.5 % glutaraldehyde in 0.1 M phosphate buffer for two hours, followed by three washes in 0.1 M phosphate buffer. After post-fixing in 1 % osmium tetroxide for 1 h, tissues were washed thrice (15 min × three times) with distilled water and serially dehydrated in 30 %-100 % ethanol for 30 min each. The tissues were infiltrated every hour once to change the mixture of 100 % acetone and Spurr resin, and once to use Spurr resin alone, followed by 8-hour incubation. Specimens of tissue were polymerized in Spurr resin for eight hours at 70 °C. Polymerized blocks were sectioned with RMC ultracut microtome (Reichert-Jung ultracut microtome) to obtain ultrathin (75 nm) cross sections. Ultrathin sections were then collected on 200 mesh copper grids and stained with 2 % Uranyl acetate and lead citrate (10 min each), washed and observed using a transmission electron microscope (TEM) JEOL 1400 (JEOL, Akishima, Japan). The ultrastructure was captured using a bottom-mounted Quamisa camera and iTEM Soft Imaging System (Soft Imaging System, Munster, Germany).

2.7. Triple antibody immuno-histochemical staining

To confirm co-localization of Bax, phosphor-p53 and cleaved caspase-3, sequential TripleStain IHC was employed using polymer-HRP and alkaline phosphatase (AP) kits to detect mouse and rabbit primary antibodies for human tissue with Permanent-Red, DAB and Emerald chromogen (#ab183286, TripleStain IHC Kit, Abcam, UK). Primary antibodies against pro-apoptotic markers included mouse Bax (1:100), mouse phosphor p53 (1:100) and rabbit cleaved caspase-3 (1:100). These antibodies were mixed each other, applied to the tissue and the incubated for 60 min. Polymer mixtures were made by adding polymer-HRP anti-mouse IgG and AP polymer anti-rabbit IgG at all are in 1:1 ratio and applied to cover each section. Unless noted otherwise, all manufacturer's instructions were followed. Finally, slides were counterstained with hematoxylin. After the slides are cleared, wipe off any extra water and let them air dry for a few seconds before dehydrating and clearing them. The tissue section was covered with 50 μL of non-aqueous mounting medium and a cover on a glass coverslip, and the images were captured by an Olympus BX53 bright field microscope using Cell Sensentry software.

2.8. Statistical analysis

The data were expressed as Mean ± Standard Error (SE) depending upon overall variable distribution. The statistical analysis was performed using Graphpad Prism 8 tools (GraphPad Software, San Diego, CA). The results were analyzed using Mann-Whitney unpaired T-test, where applicable. The *P* values obtained through Mann-Whitney unpaired T-test multiple comparison test that were less than 0.05, 0.01 & 0.001 are represented by *, **, & *** to indicate statistical significance.

3. Results

3.1. Histological analyses of human normal and KC corneas

Figs. 1 & 2 showed the histology and ultra-structural illustrations from three normal and KC corneas, respectively. Both light and electron microscopic images were revealed broken bowmen's

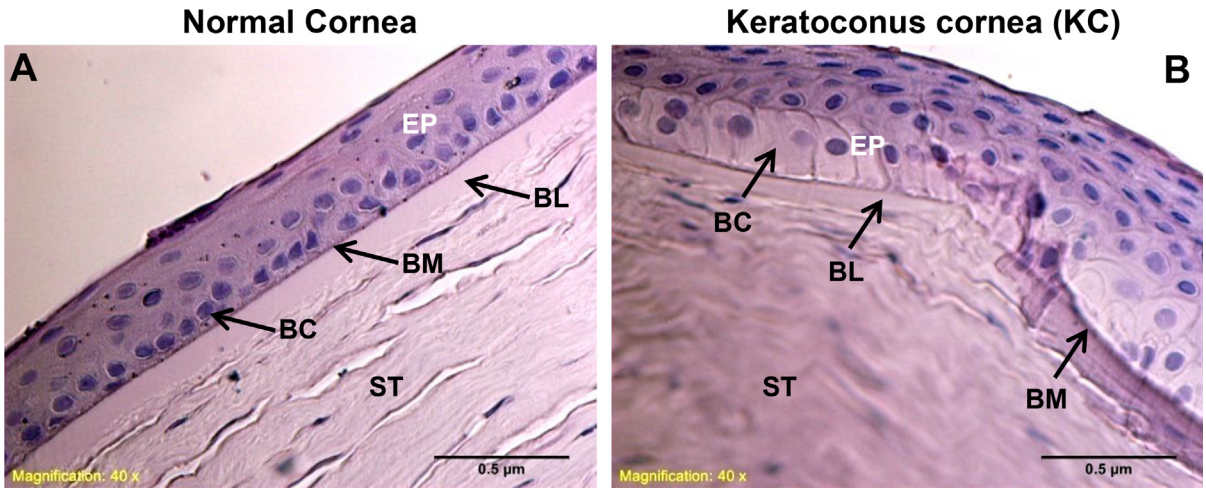

Fig. 1. Histological changes in human normal and KC corneas. As shown in (A & B), basal epithelial cells and basement membrane damage were assessed in normal and keratoconus corneas. The images were all captured at a 40x magnification. EP-epithelium, BC-basal cells, BM-basement membrane, BL-bowmen's layer, ST-stroma.

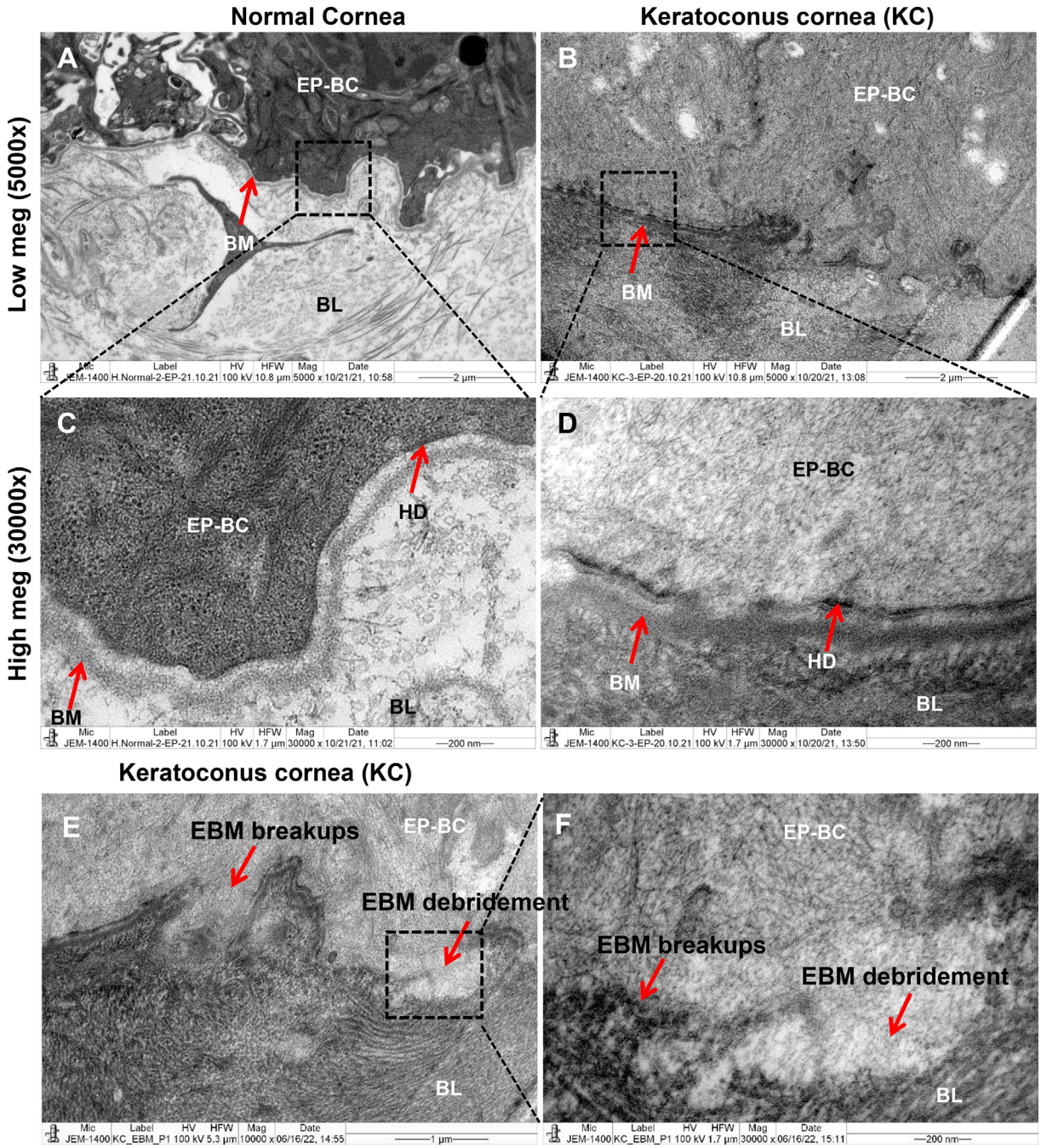

Fig. 2. Ultra-structural changes in human normal and KC corneas. The electron microscopic ultrastructural images of hemidesmosomes and basement membrane fragmentation were assessed. The (A & B) images shows in low magnification of keratoconus cornea (KC) and normal cornea (5000x). Images (C & D) show the normal and KC cornea sections at high magnification (30000x). Images (E & F) show the KC cornea sections at low (10000x) and high magnification (30000x) in basal epithelial cells basement membrane debridement's. BC-basal cells, BM-basement membrane, BL-bowmen's layer, ST-stroma, HD-hemidesmosomes, EBM-epithelial basement membrane.

layers, hemidesmosomes, and basement membrane defects on the KC corneas but not occurs in the normal corneas. Comparatively to normal corneal epithelium in H&E stain, the basal cells from KC exhibits single squamous cells in lacking nuclei (Fig. 1B). Also, the KC corneal epithelium illustrated a hallow shape with widely elongated cytosolic bodies, when compared to normal corneal epithelial cells. The high magnification images of KC corneas (Fig. 2 C, D and E, F) from electron microscopy illustrated that the epithelial basement membrane (EBM) had debridement, fragmented hemidesmosomes that were strewn throughout bowmen's layer. On both light and electron microscope images (Figs. 1 & 2), the arrow marks are indicating that the structural and ultrastructural changes in KC and normal corneal tissue sections.

3.2. Pro-apoptotic proteins expression in human normal and KC corneas

Western blot study was examined whether the expression levels of proapoptotic proteins could differ between normal and KC cornea. Immunoblotting studies were performed to determine the expression of apoptosis-associated proteins (such as Bax, Bid, Bad, p-p53 and caspases). In Fig. 3(A & B) histograms are represent-

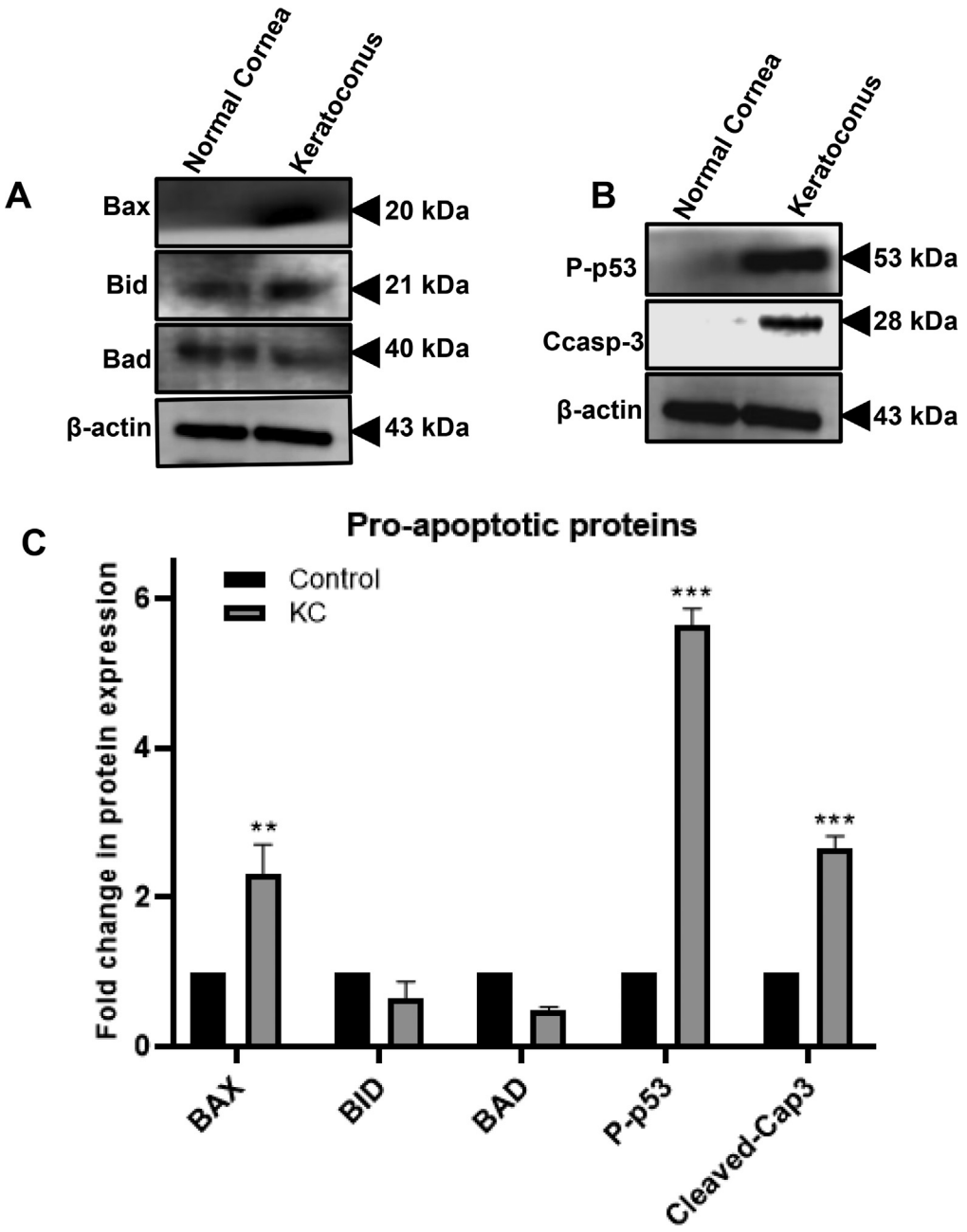

Fig. 3. Analysis of pro-apoptotic proteins expression in normal and KC corneas. Western blot images (A & B) illustrating the expression of Bax, Bid, Bad, p-p53, cleaved caspase-3, and β-actin proteins. Using Image-J software, these expressions were quantified using densitometry analysis. The graph in (C) plots shows the levels of Bax, Bid, Bad, p53, and cleaved caspase-3 protein expressions. The relative density bands of the target gene were normalized to the expression of the housekeeping gene β-actin. Three replicates were conducted for each experimental point (n = 3). The data represent Mean ± Standard Error (S.E.). Using Mann-Whitney unpaired T-test multiple comparisons, P values of 0.05, 0.01, and 0.001 representing *, **, and *** compared to normal were calculated.

ing the total protein expression of Bax, Bid, Bad, p-p53, cleaved caspase-3 and β-actin levels from three normal and KC subjects in pooled tissue samples. Fig. 3C shows the quantified results of band density using the Image-J software. In KC corneas, Bax, p-p53 and cleaved caspase-3 protein expression levels were increased significantly by 1.5, 5.6 & 2 folds ($^{*}p = 0.05$) compared with normal corneas (Fig. 3C). According to the results (Fig. 3C), the relative levels of protein expression of Bid and Bad were significantly decreased in KC cornea (more than 40 %, $^{**}p = 0.01$) as compared to normal cornea. Based on these results, corneal tissues from the KC patients showed increased caspase-3 activation, which may be contribute to enhance apoptosis.

3.3. Immuno-histochemical changes of apoptotic proteins in human normal and KC cornea

To further confirm that Bax, Bid, Bad, p-p53, and caspase-3 are associated with pro-apoptotic signaling in the normal and KC corneal epithelium, immunohistochemistry was performed (Figs. 4 and 5). The expression of pro-apoptotic proteins Bax, phospho-p53, and cleaved caspase-3 immuno-staining results indicated that the basal cells and scarred bowmen's layer of KC cornea were absolutely stained more than normal corneal epithelium (Fig. 4A-F). There was no protein expression in either the anterior or posterior stroma of the KC cornea. Comparatively, Bid and Bad proteins

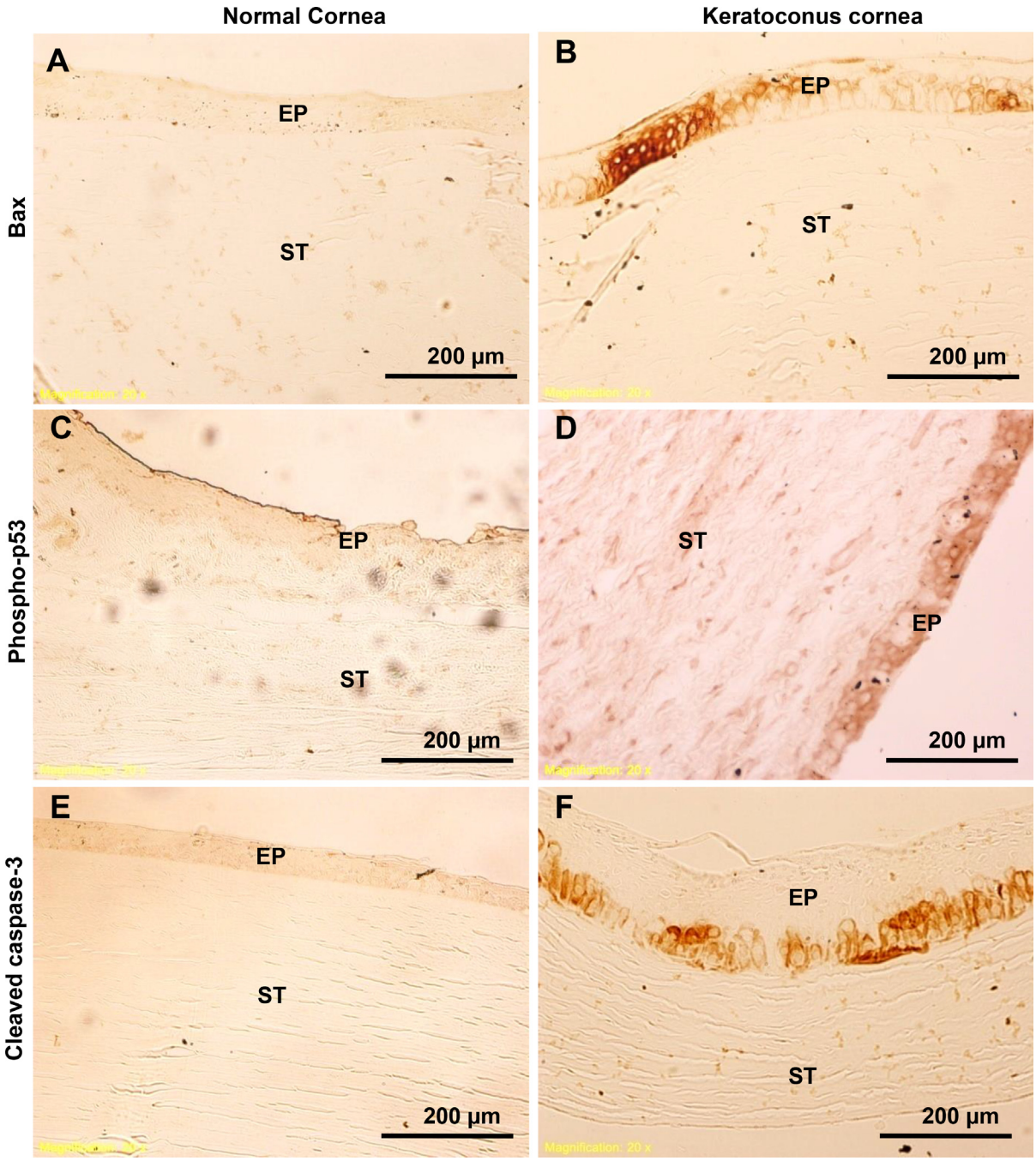

Fig. 4. Detection of pro-apoptotic proteins in human normal and KC corneas. Using immunohistochemistry, pro-apoptotic proteins Bax, phospho-p53, and cleaved caspase-3 were analyzed. Fig. 4(A-F) shows the light microscopic images of Bax, phospho-p53, and cleaved caspase-3 immunostainings in normal and KC corneal tissue sections. The images were all captured at a 20x magnification.

expressed moderately have been found in the entire scarred center epithelium of the cornea in KC (Fig. 5A-D). However, no staining was observed on the bowmen's layer, anterior and posterior stromal areas of the KC cornea. Accordingly, the immunohistochemistry staining of these three KC corneal tissue sections (Bax, phosphor-p53, and cleaved caspase-3) revealed identical results compared to normal corneal sections.

3.4. Colocalization of apoptotic proteins in human normal and KC corneas

Based on the above results, apoptosis signaling could be required to find co-localization within the KC corneal epithelium and stroma. For further confirmation, we examined whether pro-apoptotic signaling influences the expression of the apoptosis-related proteins (such as Bax, p-p53, and cleaved caspase-3). For using triple antibody staining, each antibody stain color illustration shows that mouse anti-Bax antibody interacts with mouse AP polymer to formed a permanent red chromogen, A rabbit anti-cleaved caspase-3 antibody interacts with rabbit HRP polymer to formed DAB brown chromogen and mouse p-p53 antibody interacts with mouse HRP polymer to appeared emerald green chromogen. Afterwards, a co-localization color dark blue/purple was revealed, which confirms the co-expression on the same site. The results of Fig. 6, which compares the epithelium of normal corneas (Fig. 6A) and KC corneas (Fig. 6B), indicate that the triple antibody

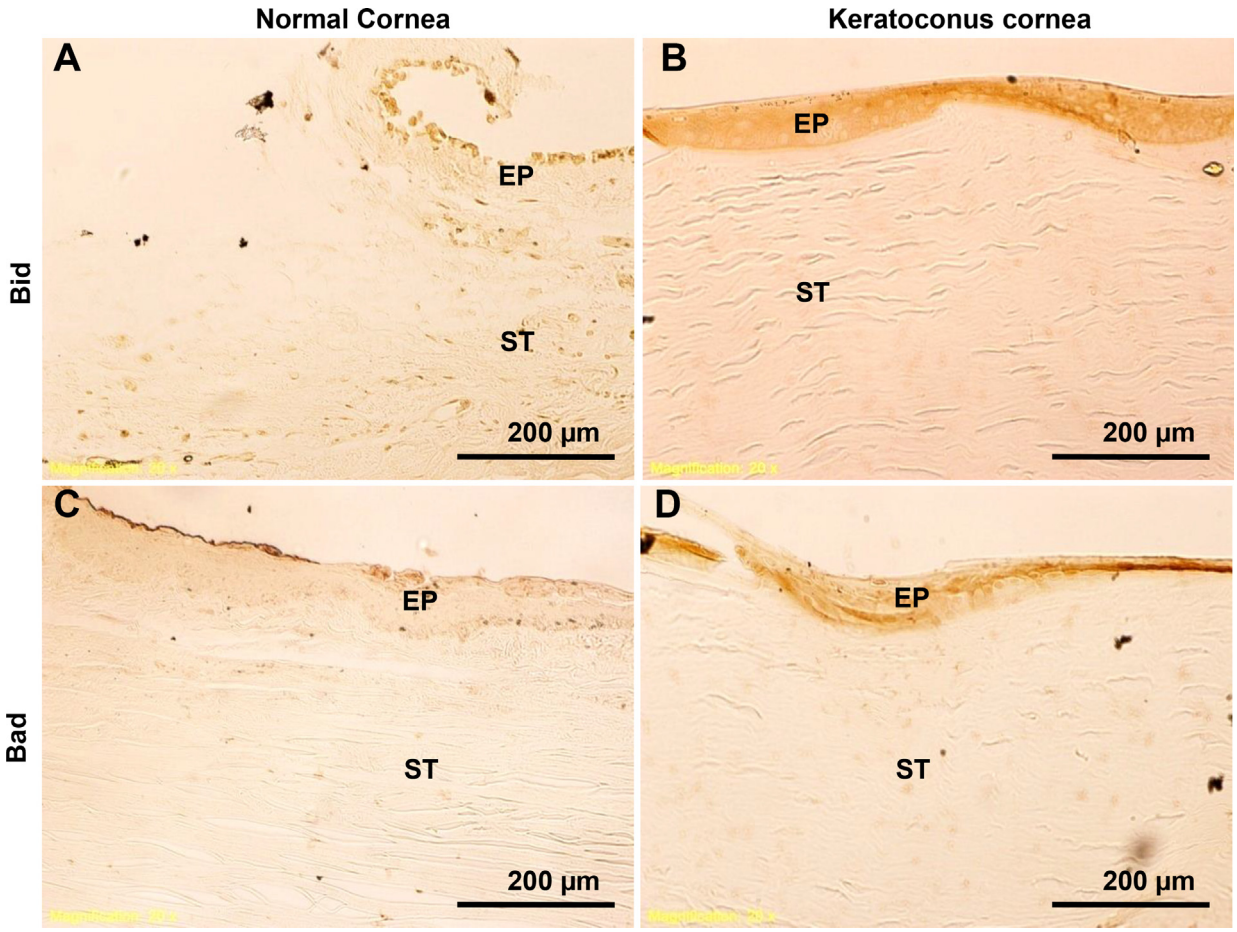

Fig. 5. Detection of pro-apoptotic proteins in human normal and KC corneas. Using immunohistochemistry, pro-apoptotic proteins Bid and Bad were analyzed. Fig. 5(A-D), immunostaining of Bad and Bid is shown in sections of normal and KC corneas. The images were all captured at a 20x magnification.

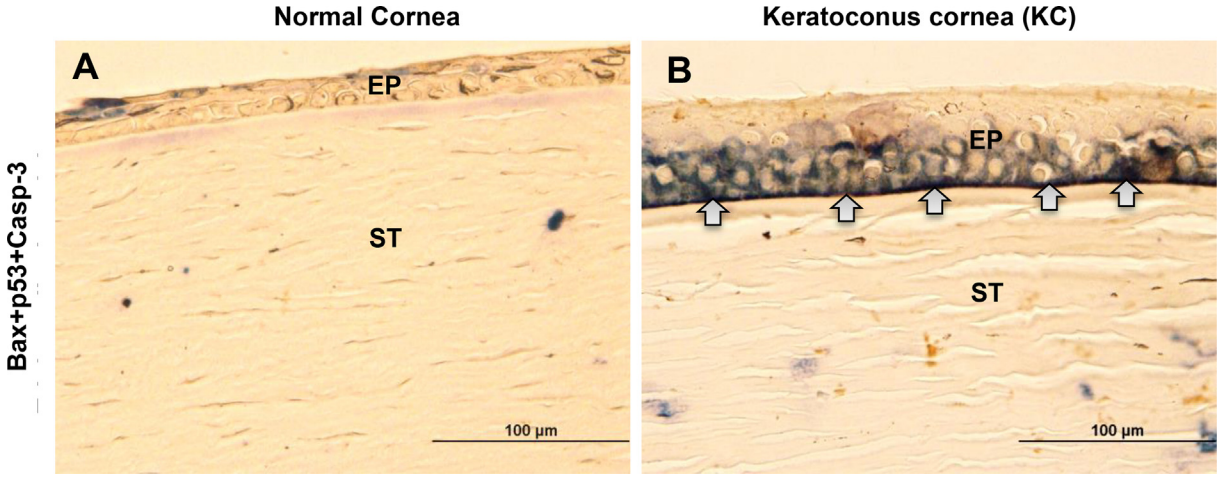

Fig. 6. An analysis of the colocalization of pro-apoptotic proteins in human normal and KC corneas. The light micrographs (A & B) show Bax, phospho-p53, and cleaved caspase-3 immunostaining in normal and KC corneal sections. The dark blue/purple color was indicating the co-localization of the triple protein's expressions (Bax, phospho-p53, and cleaved caspase-3) in normal and KC corneal tissue sections. The images were all captured at a 40x magnification.

staining illustrated strong protein colocalization (dark blue/purple) between basal cells and basement membrane on the KC corneas. On light microscope images (Fig. 6B), arrow marks indicate that the protein colocalization (dark blue/purple) from basal cells and basement membrane in KC corneal sections. Blue/purple staining was not observed in the bowmen's layer, anterior or posterior stromal areas of the KC cornea. An immuno-staining clearly shows that antibodies are expressed in the cytosolic cellular matrix and basement membrane of basal cells, but not in their nuclei. Thus, triple antibody staining of three KC corneal tissue sections (Bax, phospho-p53, and cleaved caspase-3) revealed identical results compared to normal corneal tissue sections.

3.5. Detection of progenitor cells membrane lipid content in human normal and KC cornea

The Nile red staining in cell membranes allowed us to observe membrane lipids and progenitor cell translocation in cells by using fluorescence microscopy. In Fig. 7A & B, Nile red staining revealed that in normal peripheral corneas, KC corneas had less membrane lipid content and a lower number of progenitor cells occurred. The epithelial and stromal parts of the KC cornea (Fig. 7B) differed from those of the normal cornea (Fig. 7A). The arrow marks (red colors) on fluorescence microscope images (Fig. 7A & B) indicate the presence of lipid contents in both normal and KC corneal sections. From Fig. 7C & D, the DAPI staining (blue color) supports the identification of cellular nuclei from normal and KC corneal tissue sections. In both Nile red/DAPI merged images, the deviation in membrane lipid contents and progenitor cell distribution in normal and KC corneal tissue sections are clearly showing in Fig. 7E & F. This study may help us to identify differences between the pathological changes in normal and KC corneas.

4. Discussion

Currently, there is no therapeutic target associated with the disease progression of KC, as the pathology needs to be fully

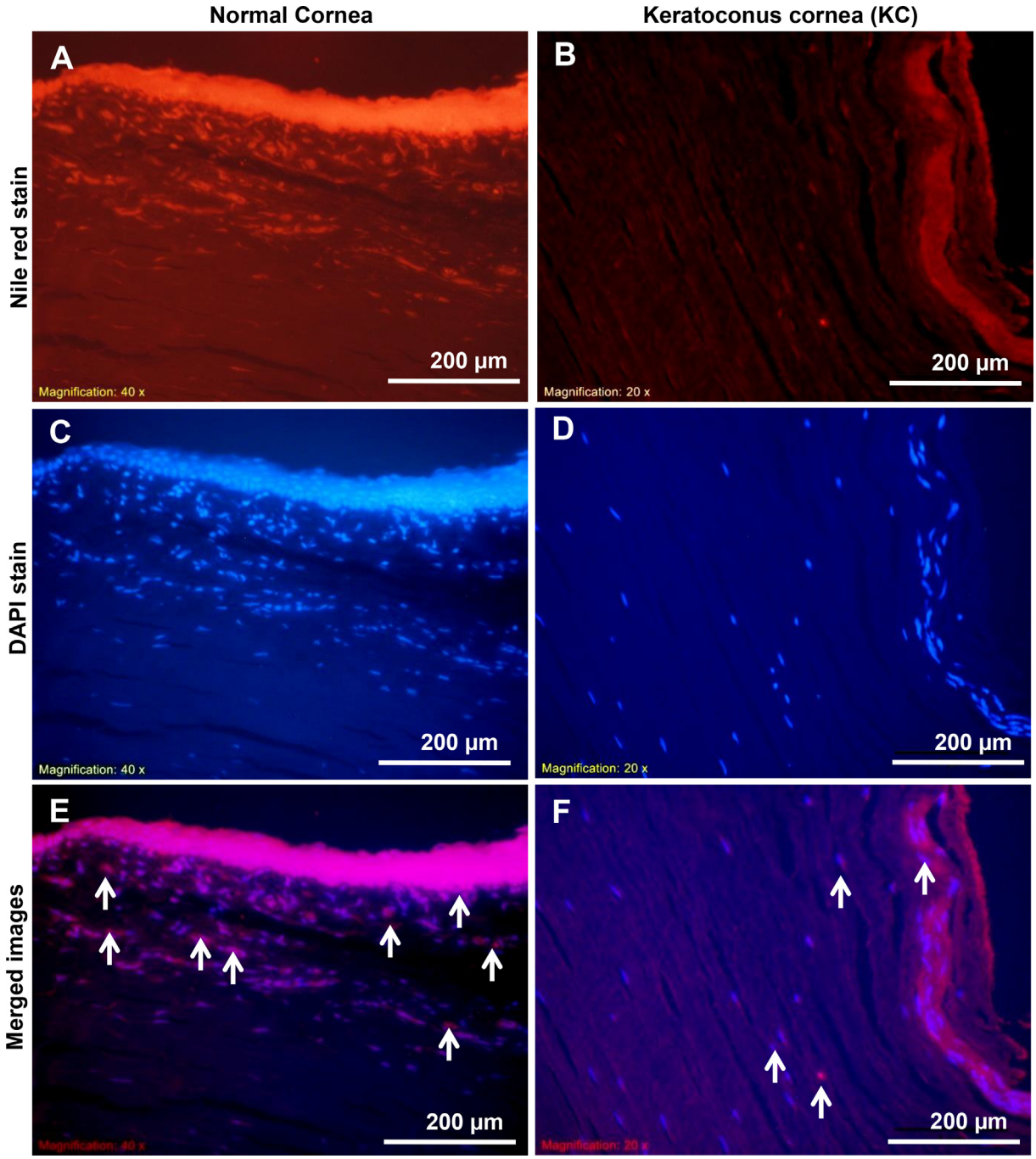

Fig. 7. Analysis of progenitor cells lipid contents in normal and KC corneal tissue sections. The (A & B) images show the fluorescent dye Nile red staining in normal and KC corneal tissue sections. The image of (C & D) shows the fluorescent dye DAPI nuclear staining in normal and KC corneal tissues. Merged fluorescent images of Nile red/DAPI staining in normal and KC corneal tissue sections is shown in (E & F). The images were all captured at a 20x magnification.

elucidated. It has been reported that certain factors contribute to the pathogenesis of KC, including genetic, metabolic, hormonal, environmental influences, oxidative stress, and cytokine signaling (Ates et al., 2021; Wojakowska et al., 2020). Also, a number of systemic diseases have been associated with an increased risk of developing KC, including, but not limited to, diabetes mellitus, connective tissue diseases, hypertension, macular edema, and autoimmune diseases (Anitha et al., 2021). The early research, it has been discovered that KC is a partially systemic disease due to the role that endocrine function plays in regulating metabolism and inflammation, some biomarkers of hormonal regulation have been projected in KC, including metabolites and hormones (McKay et al., 2016). Therefore, the identification of the key molecular players in KC-associated corneal pathogenesis may lead to new therapeutic targets to improve the therapeutic efficacy. These studies have been limited by the fact that either the whole cornea or the whole epithelium of the cornea was used.

Histopathologic changes are apparent in both the epithelium and stroma of the cornea during the progression of KC. One of the earliest detectable changes in KC cornea can be seen in its morphological changes of the corneal epithelium, as well as in other epithelial structures (Khaled et al., 2017). A few studies have also raised concerns about the extracellular matrix (ECM) that fills in the gaps of Bowmen's layer in the early stages of KC (Kenney et al., 1997; Pahuja et al., 2016). There may be a localized fibrotic repair process occurring at the sites of BM breaks based on the accumulation of proteiolytic enzymes via endocrine transductions. The combination of stromal ECM and BM may allow for both keratocytes and epithelia to perform their repair functions (Torricelli et al., 2016). In the present study, the H&E staining and electron microscopy findings illustrated that the BM is irregular shaped, accompanied by breaks in keratoconic corneas as compared to normal corneal sections (Figs. 1 and 2). These findings indicated in dysfunctional interactions between corneal epithelium and stroma, which affects gene expression as well.

In addition to the altered turnover of corneal epithelial cells, corneal thinning may also result from abnormal cell degeneration. The keratocone has a higher number of normal epithelial cells in the periphery whereas the epithelial cells at the conical apex (center) are elongated and arranged in whorls-like fashion (Sherwin & Brookes, 2004). It is generally believed that the KC cornea is primarily affected by apoptosis in the stroma and possibly in the epithelium, which leads to layers of cornea thinning. Using wound healing assays, studies have shown that apoptotic corneal epithelium can increase keratocyte death (Song et al., 2015; Coulson-Thomas et al., 2015). Also, a higher number of apoptotic cells were detected in the deeper levels of KC corneal stroma when compared to those found on the surface of normal corneas (supplementary Fig. 1). The pro-apoptotic cellular signaling mechanisms in KC are mostly unknown, except for the biomechanical, biochemical, and structural changes.

Apoptosis can also be induced by cellular stresses which act on nuclei, mitochondria, the endoplasmic reticulum or lysosomes through paracrine regulations. Despite the heterogeneity of potential cell death inducers, apoptosis exhibits common morphological and biochemical changes (Forrester et al., 2018). In addition, the IL-1 receptor, lysate products from apoptotic cells, and FAS and its ligands are all potential inducers of apoptosis (England et al., 2014; Spadea et al., 2016). In later, this family of proteins contains both pro-apoptotic Bax, Bad, and Bid and anti-apoptotic proteins Bcl2 respectively that also regulate apoptosis signals. In normal cells, Bax resides in the cytosol, but when stimulated it is translocated to the mitochondrial outer membrane. These proapoptotic proteins trigger apoptosis, which activates caspase cascade. There is no consensus on whether apoptotic cell death involves a final death pathway. In this regard, Western blots and immuno-staining were undertaken to determine the levels of apoptotic protein expressions. Based on these findings, KC corneas (Figs. 3 & 4) was overexpressed in the Bax protein, which may decline in Bid and Bad proteins expression, and it shifts to enhance p-p53 and caspase-3 proteins expression. Overall, these results indicate that increasing the pro-apoptosis protein Bax, which regulates cellular apoptosis signals, may be a key risk factor for causing cell death.

P53, another major gene, is responsible for maintaining genomic stability in biological systems (Eischen, 2016). The 53-kd phosphorprotein produced by this gene plays a role in numerous types of abnormal cell proliferation; apoptosis in response to DNA injury, as well as the prevention of replication of genomes damaged by DNA strand break (Williams & Schumacher, 2016). Only a few studies have focused on p53 subcellular expression and function in normal, mature corneal tissues. A high level of p53 protein was previously detected in the cytoplasm of normal C57BL/6 mice's corneal epithelium (Tendler & Panshin, 2020). As a consequence, pathologic p53 proteins bind to mitochondrial outer membranes, induce permeabilization of the membrane, and form complexes with proapoptotic proteins. Upon binding of these factors, cytochrome *C* is released, and caspase activation triggers apoptotic cell death (Schuler et al., 2000). Accordingly, the triple antibody immuno-staining results showed these proteins Bax-pp53-casp-3 upregulated in the cytoplasm and basal cell membrane of the KC corneal tissues sections (Fig. 6). A study published in 2013 by Tendler et al. found that p53 proteins were colocalized in various subcellular organs and induced apoptosis in cultured corneal epithelial cells after UV radiation exposure (Tendler et al., 2013). According to our knowledge, this is the first report that demonstrated the apoptotic proteins Bax-pp53-casp-3 triple antibody immuno-staining and the co-expression of apoptotic proteins in KC corneal tissues. Additionally, the Nile red fluorescent staining of the KC corneas revealed a less dense plasma membrane and smaller number of progenitor cells than those in peripheral normal corneas (Fig. 7). There were fewer progenitor cells in the epithelium and the stroma of KC corneas, and the lipid content in membrane differed from those in the normal cornea. Observations of these new findings may be helpful in understanding the pathological changes between normal and KC corneal structural integrity. By using new techniques, it will be potential to establish the clinical significance of these pro-apoptotic morphological patterns in the future. Additionally, its potential use for predicting risk factors associated with the progression of KC is to be explored.

5. Conclusions

A combination of protein expressions and histological analysis revealed structural and biological changes in KC corneal epithelia, enhancing our understanding of KC pathophysiology. As a consequence, the collective results indicate that pro-apoptotic proteins occur colocalization through basal epithelial cell damage and fragmented basement membrane, both of which enhance apoptotic induction in the KC epithelia. It has been proposed that phosphorylation of cytoplasmic p53 has a profound effect on caspase-3 activation in KC corneal epithelium and basement membrane. Further studies are needed to fully characterize the role of p53 and caspase-3 proteins and their regulation as part of the corneal epithelium of the KC. These novel findings might help to enhance our understanding of KC's apoptosis signaling pathways, thereby improving its clinical treatment and management.

Author contributions

Substantial contributions to conception and design of this study: RS, OK; Acquisition of data: RS, AAK; Analysis and interpre-

tation of data: RS, AAK; Drafting the article: RS, AIS, SAA; Revising it critically for important intellectual content: AMM, ESA, SAA; Final approval of the version to be published: RS, AMM, ESA, SAA.

Financial support

The authors are grateful to the Deanship of Scientific Research, King Saud University for funding through Vice Deanship of Scientific Research Chairs.

Declaration of Competing Interest

The authors declare that they have no known competing financial interests or personal relationships that could have appeared to influence the work reported in this paper.

Acknowledgments

The authors are grateful to thank the Researchers Support Services Unit (RSSU) from King Saud University for their technical support.

References

Alkanaan, A., Barsotti, R., Kirat, O., Khan, A., Almubrad, T., Akhtar, S., 2019. Collagen fibrils and proteoglycans of peripheral and central stroma of the keratoconus cornea - Ultrastructure and 3D transmission electron tomography. Sci. Rep. 9 (1), 19963. https://doi.org/10.1038/s41598-019-56529-1.

Amit, C., Padmanabhan, P., Narayanan, J., 2020. Deciphering the mechanoresponsive role of β-catenin in keratoconus epithelium. Sci. Rep. 10, 21382. https://doi.org/10.1038/s41598-020-77138-3.

Anitha, V., Vanathi, M., Raghavan, A., Rajaraman, R., Ravindran, M., Tandon, R., 2021. Pediatric keratoconus-Current perspectives and clinical challenges. Indian J Ophthalmol. 69 (2), 214–225. https://doi.org/10.4103/ijo.IJO_1263_20.

Atalay, E., Ozalp, O., Yıldırım, N., 2021. Advances in the diagnosis and treatment of keratoconus. Ther. Adv. Ophthalmol. 13. https://doi.org/10.1177/25158414211012796.

Ates, K.M., Estes, A.J., Liu, Y., 2021. Potential underlying genetic associations between keratoconus and diabetes mellitus. Adv. Ophthalmol. Pract. Res. 1 (1). https://doi.org/10.1016/j.aopr.2021.100005.

Atilano, S.R., Lee, D.H., Fukuhara, P.S., Chwa, M., Nesburn, A.B., Udar, N., Kenney, M. C., 2019. Corneal oxidative damage in keratoconus cells due to decreased oxidant elimination from modified expression levels of SOD enzymes, PRDX6, SCARA3, CPSF3, and FOXM1. J Ophthalmic. Vis. Res. 14 (1), 62–70. https://doi.org/10.4103/jovr.jovr_80_18.

Chaerkady, R., Shao, H., Scott, S.G., Pandey, A., Jun, A.S., Chakravarti, S., 2013. The keratoconus corneal proteome: loss of epithelial integrity and stromal degeneration. J Proteomics. 87, 122–131. https://doi.org/10.1016/j.jprot.2013.05.023.

Chwa, M., Atilano, S.R., Reddy, V., Jordan, N., Kim, D.W., Kenney, M.C., 2006. Increased stress-induced generation of reactive oxygen species and apoptosis in human keratoconus fibroblasts. Invest. Ophthalmol. Vis. Sci. 47 (5), 1902–1910. https://doi.org/10.1167/iovs.05-0828.

Coulson-Thomas, V.J., Chang, S.H., Yeh, L.K., Coulson-Thomas, Y.M., Yamaguchi, Y., Esko, J., Liu, C.Y., Kao, W., 2015. Loss of corneal epithelial heparan sulfate leads to corneal degeneration and impaired wound healing. Invest. Ophthalmol. Vis. Sci. 56 (5), 3004–3014. https://doi.org/10.1167/iovs.14-15341.

Eischen, C.M., 2016. Genome stability requires p53. Cold Spring Harb. Perspect. Med. 6, (6). https://doi.org/10.1101/cshperspect.a026096 a026096.

England, H., Summersgill, H.R., Edye, M.E., Rothwell, N.J., Brough, D., 2014. Release of interleukin-1α or interleukin-1β depends on mechanism of cell death. J Biol. Chem. 289 (23), 15942–15950. https://doi.org/10.1074/jbc.M114.557561.

Forrester, S.J., Kikuchi, D.S., Hernandes, M.S., Xu, Q., Griendling, K.K., 2018. Reactive oxygen species in metabolic and inflammatory signaling. Circ. Res. 122 (6), 877–902. https://doi.org/10.1161/CIRCRESAHA.117.311401.

Grieve, K., Georgeon, C., Andreiuolo, F., Borderie, M., Ghoubay, D., Rault, J., Borderie, V.M., 2016. Imaging microscopic features of keratoconic corneal morphology. Cornea. 35 (12), 1621–1630. https://doi.org/10.1097/ICO.0000000000000979.

Hashmani, S., Hashmani, N., Memon, R.S., 2017. Corneal collagen cross-linking combined with an artiflex iris-fixated anterior chamber phakic intraocular lens implantation in a patient with progressive keratoconus. Case Rep. Ophthalmol. 8 (3), 482–488. https://doi.org/10.1159/000480728.

Jumabay, M., Zhang, R., Yao, Y., Goldhaber, J.I., Bostrom, K.I., 2010. Spontaneously beating cardiomyocytes derived from white mature adipocytes. Cardiovasc. Res. 85 (1), 17–27. https://doi.org/10.1093/cvr/cvp267.

Kaluzhny, Y., Kinuthia, M.W., Lapointe, A.M., Truong, T., Klausner, M., Hayden, P., 2020. Oxidative stress in corneal injuries of different origin: Utilization of 3D human corneal epithelial tissue model. Exp. Eye Res. 190,. https://doi.org/10.1016/j.exer.2019.107867 107867.

Kammergruber, E., Rahn, C., Nell, B., Gabner, S., Egerbacher, M., 2019. Morphological and immunohistochemical characteristics of the equine corneal epithelium. Vet. Ophthalmol. 22 (6), 778–790. https://doi.org/10.1111/vop.12651.

Kenney, M.C., Nesburn, A.B., Burgeson, R.E., Butkowski, R.J., Ljubimov, A.V., 1997. Abnormalities of the extracellular matrix in keratoconus corneas. Cornea. 16 (3), 345–351. PMID: 9143810.

Khaled, M.L., Helwa, I., Drewry, M., Seremwe, M., Estes, A., Liu, Y., 2017. Molecular and histopathological changes associated with keratoconus. Biomed. Res. Int. 2017, 7803029. https://doi.org/10.1155/2017/7803029.

Li, Y., Xu, Z., Liu, Q., Wang, Y., Lin, K., Xia, J., Chen, S., Hu, L., 2021. Relationship between corneal biomechanical parameters and corneal sublayer thickness measured by Corvis ST and UHR-OCT in keratoconus and normal eyes. Eye Vis. (Lond) 8 (1), 2. https://doi.org/10.1186/s40662-020-00225-z.

Liu, R., Yan, X., 2018. Sulforaphane protects rabbit corneas against oxidative stress injury in keratoconus through activation of the Nrf-2/HO-1 antioxidant pathway. Int. J Mol. Med. 42 (5), 2315–2328. https://doi.org/10.3892/ijmm.2018.3820.

Marino, G.K., Santhiago, M.R., Santhanam, A., Lassance, L., Thangavadivel, S., Medeiros, C.S., Bose, K., Tam, K.P., Wilson, S.E., 2017. Epithelial basement membrane injury and regeneration modulates corneal fibrosis after pseudomonas corneal ulcers in rabbits. Exp. Eye Res. 161, 101–105. https://doi.org/10.1016/j.exer.2017.05.003.

Masiwa, L.E., Moodley, V., 2020. A review of corneal imaging methods for the early diagnosis of pre-clinical Keratoconus. J Optom. 4, 269–275. https://doi.org/10.1016/j.optom.2019.11.001.

McKay, T.B., Hjortdal, J., Sejersen, H., Asara, J.M., Wu, J., Karamichos, D., 2016. Endocrine and metabolic pathways linked to keratoconus: implications for the role of hormones in the stromal microenvironment. Sci. Rep. 6, 25534. https://doi.org/10.1038/srep25534.

Mobaraki, M., Abbasi, R., Omidian Vandchali, S., Ghaffari, M., Moztarzadeh, F., Mozafari, M., 2019. Corneal repair and regeneration: current concepts and future directions. Front Bioeng. Biotechnol. 7, 135. https://doi.org/10.3389/fbioe.2019.00135.

Pahuja, N., Kumar, N.R., Shroff, R., Shetty, R., Nuijts, R.M., Ghosh, A., Sinha-Roy, A., Chaurasia, S.S., Mohan, R.R., Ghosh, A., 2016. Differential molecular expression of extracellular matrix and inflammatory genes at the corneal cone apex drives focal weakening in keratoconus. Invest. Ophthalmol. Vis. Sci. 57 (13), 5372–5382. https://doi.org/10.1167/iovs.16-19677.

Schuler, M., Bossy-Wetzel, E., Goldstein, J.C., Fitzgerald, P., Green, D.R., 2000. p53 induces apoptosis by caspase activation through mitochondrial cytochrome c release. J Biol. Chem. 275 (10), 7337–7342. https://doi.org/10.1074/jbc.275.10.7337.

Sherwin, T., Brookes, N.H., 2004. Morphological changes in keratoconus: pathology or pathogenesis. Clin. Exp. Ophthalmol. 32 (2), 211–217. https://doi.org/10.1111/j.1442-9071.2004.00805.x.

Shetty, R., Sharma, A., Pahuja, N., Chevour, P., Padmajan, N., Dhamodaran, K., Jayadev, C., Nuijts, R.M.M.A., Ghosh, A., Nallathambi, J., Trajkovic, V., 2017. Oxidative stress induces dysregulated autophagy in corneal epithelium of keratoconus patients. PLoS One 12 (9). https://doi.org/10.1371/journal.pone.0184628.

Song, X., Stachon, T., Wang, J., Langenbucher, A., Seitz, B., Szentmary, N., 2015. Viability, apoptosis, proliferation, activation, and cytokine secretion of human keratoconus keratocytes after cross-linking. Biomed. Res. Int. 2015, 254237. doi: 10.1155/2015/254237.

Spadea, L., Giammaria, D., Trabucco, P., 2016. Corneal wound healing after laser vision correction. Br. J Ophthalmol. 100 (1), 28–33. https://doi.org/10.1136/bjophthalmol-2015-306770.

Tendler, Y., Panshin, A., 2020. Features of p53 protein distribution in the corneal epithelium and corneal tear film. Sci Rep. 10 (1), 10051. https://doi.org/10.1038/s41598-020-67206-z.

Tendler, Y., Pokroy, R., Panshin, A., Weisinger, G., 2013. p53 protein subcellular localization and apoptosis in rodent corneal epithelium cell culture following ultraviolet irradiation. Int. J Mol. Med. 31 (3), 540–546. https://doi.org/10.3892/ijmm.2013.1247.

Torricelli, A.A., Santhanam, A., Wu, J., Singh, V., Wilson, S.E., 2016. The corneal fibrosis response to epithelial-stromal injury. Exp. Eye Res. 142, 110–118. https://doi.org/10.1016/j.exer.2014.09.012.

Vazirani, J., Basu, S., 2013. Keratoconus: current perspectives. Clin. Ophthalmol. 7, 2019–2030. https://doi.org/10.2147/OPTH.S50119.

Williams, A.B., Schumacher, B., 2016. p53 in the DNA-damage-repair process. Cold Spring Harb. Perspect. Med. 6, (5). https://doi.org/10.1101/cshperspect.a026070 a026070.

Wojakowska, A., Pietrowska, M., Widlak, P., Dobrowolski, D., Wylęgała, E., Tarnawska, D., 2020. Metabolomic signature discriminates normal human cornea from keratoconus-a pilot GC/MS study. Molecules 25 (12), 2933. https://doi.org/10.3390/molecules25122933.

Wojcik, K.A., Kaminska, A., Blasiak, J., Szaflik, J., Szaflik, J.P., 2013. Oxidative stress in the pathogenesis of keratoconus and Fuchs endothelial corneal dystrophy. Int. J Mol. Sci. 14 (9), 19294–19308. https://doi.org/10.3390/ijms140919294.

Yam, G.H., Fuest, M., Zhou, L., Liu, Y.C., Deng, L., Chan, A.S., Ong, H.S., Khor, W.B., Ang, M., Mehta, J.S., 2019. Differential epithelial and stromal protein profiles in cone and non-cone regions of keratoconus corneas. Sci. Rep. 9 (1), 2965. https://doi.org/10.1038/s41598-019-39182-6.

You, J., Corley, S.M., Wen, L., Hodge, C., Hollhumer, R., Madigan, M.C., Wilkins, M.R., Sutton, G., 2018. RNA-Seq analysis and comparison of corneal epithelium in keratoconus and myopia patients. Sci. Rep. 8 (1), 389. https://doi.org/10.1038/s41598-021-98363-4.